

# EXPERIMENTAL RELATIONSHIP BETWEEN LAND USE/LAND COVER AND UNDERGROUND FLOW IN AL BA COMMUNE IN THE CENTRAL REGION OF VIETNAM

Ha NGUYEN-NGAN<sup>1\*</sup>, Huong TRAN-THI THU<sup>1</sup>, Binh PHAM-QUOC<sup>1</sup>, Van TRAN-THI<sup>2,3</sup>, & Vinh PHAM-THE<sup>1</sup>

<sup>1</sup>*Southern Institute of Water Resources Research (SIWRR), Ho Chi Minh City, 70000, Vietnam*

<sup>2</sup>*Faculty of Environment and Natural Resources, Ho Chi Minh City University of Technology (HCMUT), 268 Ly Thuong Kiet Street, District 10, Ho Chi Minh City, Vietnam*

<sup>3</sup>*Vietnam National University Ho Chi Minh City, Linh Trung Ward, Thu Duc District, Ho Chi Minh City, Vietnam*

\* Corresponding author: nganha97@hotmail.com

**Abstract:** Rapid urbanization and intensive agricultural practices in Vietnam's Central Highlands have substantially transformed land use/land cover (LULC) patterns, with implications for groundwater resources necessitating measurement. The objective of this investigation is to examine the links between multi-temporal variations in LULC and changes in underground water flow in Al Ba Commune, Gia Lai Province. Supervised object-based classification of Landsat and Sentinel imagery from the past 25 years has produced consistent LULC maps as inputs for the model. Geospatial data of LULC, meteorological data, and in-situ data of groundwater flow (Q) were used to calibrate and validate the integrated hydrological MIKE SHE model and simulate past Q conditions for correlation analysis. With these data on LULC and groundwater flow, this study investigates the relationship between LULC changes and Q using Multivariate Linear Regression (MLR) and Ridge Regression models. The MLR model showed high R<sup>2</sup> (0.91) but positive impacts of all LULC classes on Q, contrary to expectations. Further analysis with Variance Inflation Factor (VIF) revealed multicollinearity among LULC variables, which was addressed using Ridge Regression with a bias factor to correct for this issue. The revised model demonstrated that non-vegetative covers negatively affect Q while vegetative covers have a positive impact. These results highlight the complex dynamics of LULC changes on groundwater resources, which can be detected by statistical approaches. The results of study could be important for sustainable land management.

**Keywords:** LULC, groundwater flow, MIKE SHE model, object-based classification, multiple regression

## 1. INTRODUCTION

Groundwater, the fundamental life-sustaining earthly resource is increasingly fraught with demand due to escalating population numbers, burgeoning urban growth and intensifying agricultural practices (El-Khoury, 2022; Salem et al., 2023). Such dynamics are propelling rapid modifications in land use/land cover (LULC) within human timelines (Ansari et al., 2016; Siddik et al., 2022a; Al-Kindi et al., 2023). Anthropogenic interference has significantly impacted nature's recharging mechanisms along with patterns of subterranean

water flow cycle too (Scanlon et al., 2005; Han et al., 2017; Mojid & Mainuddin, 2021; Siddik et al., 2022a). Further compounding this quandary is precipitous exhaustion occurring from over-extraction of groundwater – a phenomenon visible across diverse global landscapes as India (Hussain, 2022; Koshy, 2023), China (Lancia et al., 2022; Wang et al., 2022; Huang et al., 2023) or the United States (USGS, 2018; O'Neill et al., 2023) amongst others (Fienen & Arshad, 2016; González-Trinidad et al., 2017; El-Khoury, 2022).

In the context of Vietnam, groundwater resources play a vital role in supporting various sectors such as agriculture, industry and domestic use

in many parts of the country. The groundwater resources in Vietnam are currently at risk of depletion and severe pollution (VWSA, 2022). This situation is apparent in the Central Highlands region, known for its abundant natural resources and socioeconomic potential, which is facing significant challenges due to the lack of water resources in areas with scarce water supply (DWRM, 2015; Phong, 2020; Nguyen et al., 2021). Provinces such as Dak Lak, Gia Lai, Kon Tum, Dak Nong, and Lam Dong have been unknowingly using groundwater sources without proper planning, leading to reduced groundwater availability during the annual dry season (DWRM, 2015). The region's forests are also suffering destruction due to factors such as decreasing rainfall and prolonged dry seasons. The high demand for irrigation water, particularly for long-term industrial crops like coffee and pepper, has led to the extensive and unregulated utilization of underground water sources, resulting in uncertain outcomes and perforations, contributing to groundwater depletion in the region (Dan, 2016; Nguyen et al., 2021; VAWR, 2021).

It is apparent from the mentioned contexts that urbanization is leading to the constant conversion of forests and vegetated regions into farmland, cities, and industrial areas. Each of these transformations has diverse impacts on the recharge rates of groundwater (Baker & Miller, 2013; Kuroda et al., 2017; El-Khoury, 2022; Siddik et al., 2022a). Thus, the quantification of the effects of changes in land cover on groundwater sources and the formulation of well-informed groundwater management policies is one of the rational actions (El-Khoury, 2022; Al-Kindi et al., 2023). and it plays a crucial role in contributing to Sustainable Development Goal 6 of the United Nations (Mensah et al., 2022).

Extensive research has been conducted to understand the impact of LULC changes on various aspects of groundwater systems, including recharge rates (Devi et al., 2020; Siddik et al., 2022a; Salem et al., 2023), water table levels (Elmahdy et al., 2020; El-Khoury, 2022; Salem et al., 2023), and quality of groundwater (Mondal et al., 2020; Ahmad et al., 2021; Yadav & Yadav, 2023). These studies have applied a range of methodologies and technological tools to assess the influence of LULC alterations on groundwater resources. Among these, the MIKE SHE hydrological model has emerged as a particularly effective tool in capturing the complexities of groundwater response to LULC changes over time (Im et al., 2009; Wijesekara et al., 2010; Ma et al., 2016; Salem et al., 2023). This model uses a physics-based integrated catchment modelling system to describe in detail the structure of the unsaturated and

saturated zones below the ground surface, effectively dividing them into different soil layers. This allows the integration of comprehensive land cover, terrain, hydrometeorological and soil data to provide integrated modellings of catchment hydrology such as precipitation, infiltration, surface water flow, groundwater flow, recharge and evapotranspiration processes (Sandu & Virsta, 2015; Prucha et al., 2016; MIKE SHE, 2023). The ability of the MIKE SHE model to simulate interconnected hydrological processes has made it invaluable for analysing the impacts of land cover on groundwater flow (Keilholz et al., 2015; Ma et al., 2016; Duranel et al., 2021; Salem et al., 2023). Despite previous efforts using MIKE SHE and remote sensing to assess these impacts (Wijesekara et al., 2010; Keilholz et al., 2015; Shu et al., 2018), a definitive link between land cover changes and groundwater dynamics remains to be established. The hypothesis is that transformations in land cover classes will correlate significantly with fluctuations in groundwater flow. The results are expected to quantify and evaluate the impacts of different LULC-type changes on groundwater flows.

This study aims to explore the relationship between land cover changes and groundwater flow in Al Ba Commune, Chu Se District, Gia Lai Province, Vietnam, from 1988 to 2022, by using the MIKE SHE model combined with object-based land cover classifications from multi-temporal satellite imagery (Landsat 5-LST5, Landsat 8-LST8, Sentinel 2A-S2A). It involves generating land cover maps, simulating past groundwater conditions with the MIKE SHE model, and applying regression model to quantify the impact of land cover changes on groundwater. The expected outcome is to better understand this relationship to support sustainable groundwater management and informed land use planning in the region.

## 2. MATERIALS AND METHODS

### 2.1 Study area

The selected pilot area is located along Provincial Road 438 in Al Ba Commune, Chu Se District, Gia Lai Province, Vietnam. It covers an area of approximately 290 hectares and includes various terrains such as bare soil, residential areas, cultivated land, and wetlands. The pilot area is mostly composed of weathered basaltic soils that have undergone substantial weathering procedures.

The pilot area resides in a highland tropical monsoon climate region featuring substantial humidity levels and precipitations. Typhoon occurrences are a rare phenomenon within this

locality. The climate is separated into two primary seasons, the rainy and dry seasons. The rainy season normally persists from May to October, while the dry season extends between November and April of the following year. The yearly temperature ranges from 22 to 25°C, and the average annual precipitation ranges from 1,750-2,500 mm.

The Al Ba water system comprises the main Ia Pal tributary, named Ia Hboong stream, which is approximately 29 km in length. The flow direction is from northwest to southeast, passing through the Phu Thien district before flowing into the Ba River. The location of the spring in the pilot area was determined by flow measurement and geological structure survey using three boreholes. Figure 1 describes the study area.

## 2.2 Materials

### 2.2.1 Data on natural conditions

In connection with the groundwater flow simulation, we provide a more detailed insight into the geological data and the groundwater table. Geological data was collected by conducting measurements and surveys at three drilling sites

within the study basin (see Figure 1-d). Each borehole was drilled to a depth of approximately 45 m. The predominant geological formation comprises basaltic volcanic deposits in the Pliocene-Pleistocene formation, which has been divided into four distinct layers (see Figure 2). The dimensional distribution of the geological strata in the pilot basin is shown in this data. Four layers of soil profile were determined from the boreholes.

The depth of the groundwater table (see Figure 3) shows that the groundwater flow direction is concentrated towards borehole LK1. This borehole is close to the spring of the pilot basin and is also the lowest point of water accumulation in the basin. Based on the horizontal extent of the groundwater table (refer to Figure 4), the elevation of the groundwater level (blue line) changes according to different positions on the cross-section of the groundwater table. The depth of the underground water level gradually decreases as it approaches the spring location, from LK3 to LK1.

To summarise the section materials, Table 1 synthesises all inputs into three models: (1) MIKE SHE model; (2) LULC classification model; and (3) Multivariate regression model.

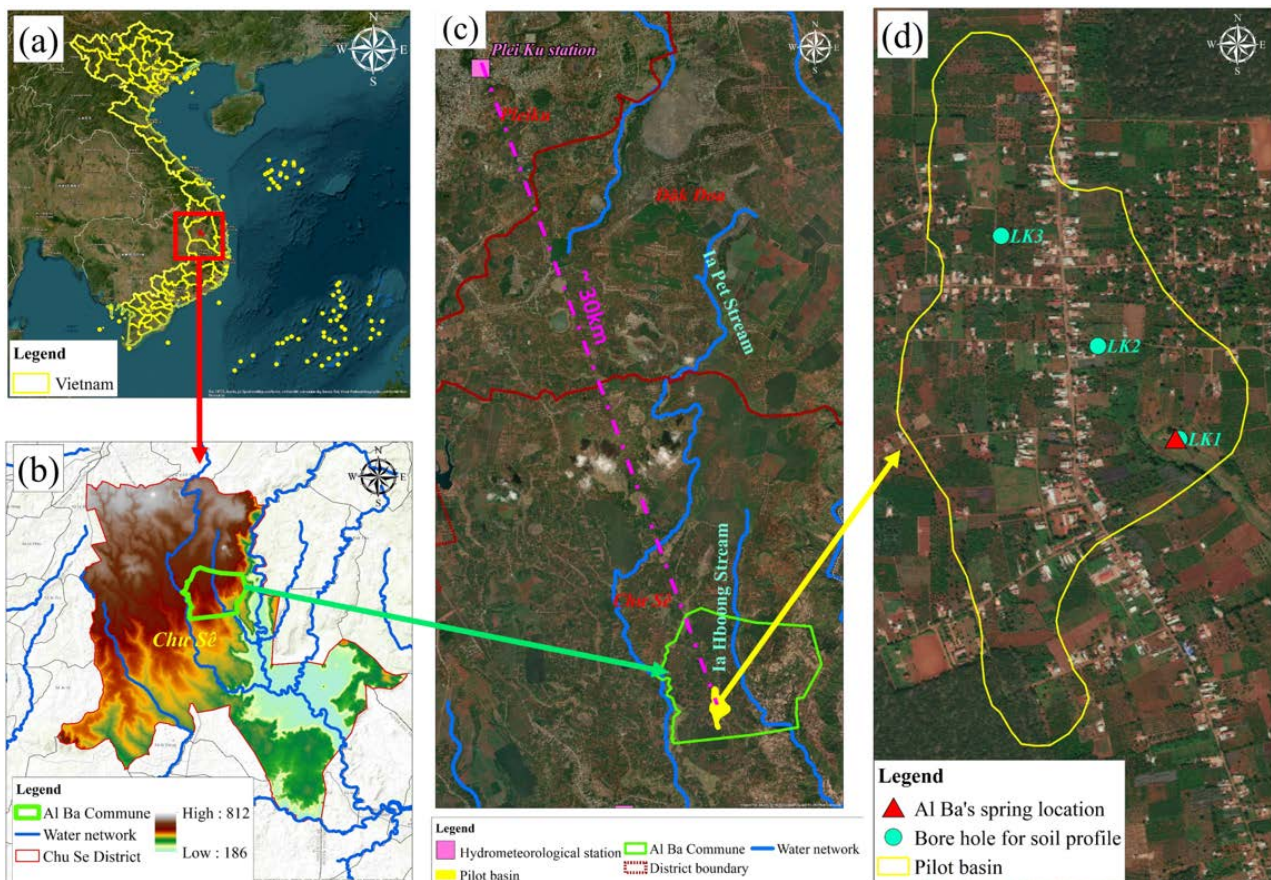


Figure 1. (a) Vietnam on Google Earth; (b) Chu Se District with 10 m DEM; (c) Al Ba Commune and location of hydro-meteorological station; (d) Pilot basin location with boreholes for soil profile measurement and spring location

Depth	LK1 (m)	LK2 (m)	LK3 (m)	Soil Description
05				Layer 1: The Bazan soil is completely weathered into brownish-red clay. It has a weak and soft structure.
10				
15				Layer 2: The Bazan soil is partially weathered, appearing as small, fragmented clumps with a grayish-blue color.
20				
25	22.0			Layer 3: The Bazan soil has pore spaces, characterized by a grayish ash color. The pore space accounts for 15-20% of the soil volume, with pore diameters ranging from 2-8mm. The connectivity between pore spaces is poor, and the rock exhibits relatively strong cracking and fissuring.
	22.8			
30		28.0		
35	31.8	30.4	31.7	Layer 4: The Bazan soil is compacted, featuring a dark gray silt. The rock is relatively hard and shows minimal cracking or fissuring.
40		33.4	35.2	
45	45.0	45.0	45.0	

Figure 2. Geological layers at three boreholes

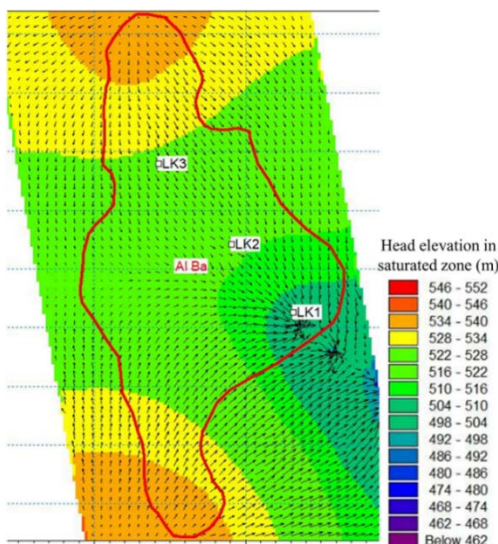


Figure 3. Direction of groundwater flow in the pilot basin

## 2.3 Methods

### 2.3.1 LULC classification

Before obtaining the LULC information from the aforementioned remote sensing images, these images underwent pre-processing procedures. The pre-processing procedures included (i) radiometric calibration, (ii) geometry adjustment, and (iii) scaling to match the dimensions of the research area. The objective of these procedures was to consolidate the input data for the LULC categorization.

The supervised object-based image analysis (OBIA) method was utilized for the image interpretation of LULC classification (see Figure 5). The proposed approach uses a segmentation procedure to group adjacent pixels based on their commonalities in color and form features. This

involves calculating the mean pixel values and integrating geographic data. The utilization of segmented objects in the images provides a more accurate representation of real-world properties, leading to improved classification outcomes (ESRI, 2023).

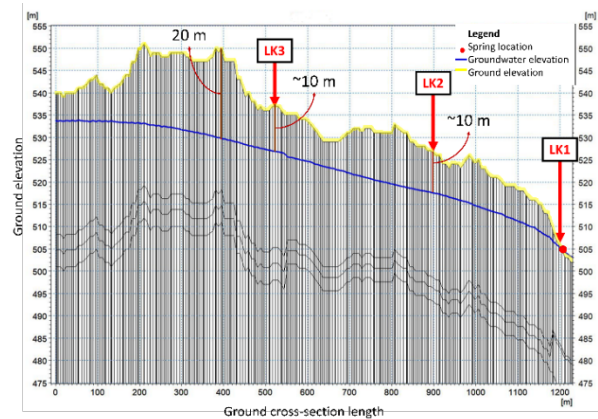


Figure 4. Simulated groundwater level line (horizontal extent passing through LK1-LK2-LK3)

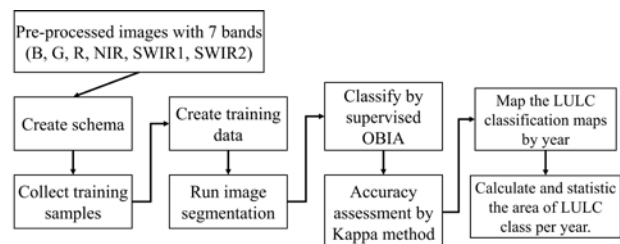


Figure 5. Workflow of supervised OBIA

In the schema creation stage, six classes were established based on the features of the pilot area. These classes consist of bare soil, built-up areas, cropland, forest, rangeland, and wetland. Each class is characterized as (1) Bare soil refers to soil that is devoid of vegetation and has no specific usage; (2) The built-up area encompasses residential and commercial areas, as well as roads, paved with concrete that lack vegetation; (3) Cropland is agricultural land used for growing crops. In the research field, cropland is predominantly utilized for cultivating arid crops such as upland rice, perennial crops, including coffee and pepper, and short-term crops such as hybrid maize, peanuts, and sesame; (4) Forest encompass planted woodlands that have diverse purposes, such as production, conservation, or special use, and comprise of trees such as eucalyptus and acacia; (5) Rangeland open and uncultivated lands used for livestock grazing; (6) Wetland primarily occur in the form of paddy fields, undeveloped land that retains water, and to a lesser extent, dry river and streambeds.

Table 1. The required input data

Model	Input	Sources	Descriptions
<b>MIKE SHE ground-water model</b>	DEM 10m x 10m	ESA-ALOS PALSAR	The current topography of the pilot area can be simulated using the DEM, which ranges from +276 to +653 metres. The terrain in the study area slopes steeply from north to south.
	Geological data at 3 boreholes	From this research's surveys and measurements	Describe the distribution of geological layers in the pilot area in terms of their dimensions.
	Precipitation & Evapotranspiration data	The real-time daily measurements recorded at the Pleiku station	The station is in Gia Lai province with the data spanning from 1988 to 2022. Represent the meteorological conditions the pilot area, spanning from 1980 to 2022.
	Leaf Area Index (LAI)	Calculated from LULC data	The LAI, or total leaf area per unit of land area, is used to assess plant light absorption and water evaporation capacity, calculated using the Specific Leaf Area Vegetation Index (SLAVI) by Lymburner et al., (2000). LAI of each LULC class: Baresoil & built-up area (0), cropland (1.05), forest (1.18), rangeland (0.63), wetland (1.05).
	Root depth	From this research's surveys with local authorities and research of Bouillet et al., (2023)	The data show how different plant roots penetrate the earth, affecting water absorption. Bare soil and built-up areas have no root depth. Root depth of each LULC class: Baresoil & built-up area (0 m), cropland (0.6 m), forest (2 m), rangeland (0.3 m), wetland (0.9 m).
	In-situ measured groundwater flows	From this research's surveys and measurements	In-situ groundwater flow data measured at the spring locations were gathered in 5 phases between 2021 & 2022 to calibrate & validate the MIKE SHE model.
<b>LULC classification model</b>	Satellite images (LST5, LST8, S2A)	USGS EarthExplorer (LST5, LST 8); Copernicus browser (S2A)	Satellite images from 1988 to 2022 were used to derive LULC data for the study area. The highest quality images are selected, with a 10% cloud cover threshold. The model includes 25 years from 1988 to 2022, with LST5 images from 1988 to 2011, LST8 images from 2014 and 2015, and S2A images from 2016 to 2022.
	Digital maps	Local authorities	Local authorities' LULC maps have been collected for years to support satellite image classification, with overlapping VN-2000 coordinate system maps used for processing.
<b>Multivariate regression model</b>	Simulated groundwater flows	Data from MIKE SHE groundwater model.	The regression model was developed using 1988-2018 simulated groundwater flow data at the spring location & validated using 2019-2022.
	Area of each LULC type by years	The data were extracted from the LULC classification model from 1988-2022	The data were extracted from the LULC classification model from 1988-2022, with 1988-2018 for regression model development & 2019-2022 for model validation.

### 2.3.2 Simulation specification of MIKE SHE model

The MIKE SHE model is constructed to simulate integrated processes of overland flow, unsaturated flow, saturated flow, and evaporation through vegetation cover.

(a) To describe natural surface water movement, the Overland Flow module of MIKE SHE solves the Saint Venant equations using the diffusion wave approximation (DHI, 2023). Overland flow simulates the movement of ponded surface water across the topography. It was simulated using the Simplified Overland Flow Routing method.

(b) The flow in the saturation zone of the MIKE SHE model is expressed by Darcy's three-dimensional flow equation (DHI, 2023):

$$\frac{\partial}{\partial x} \left( K_{xx} \frac{\partial h}{\partial x} \right) + \frac{\partial}{\partial y} \left( K_{yy} \frac{\partial h}{\partial y} \right) + \frac{\partial}{\partial z} \left( K_{zz} \frac{\partial h}{\partial z} \right) - Q = S_s \frac{\partial h}{\partial t} \quad (1)$$

where,  $K_{xx}$ ,  $K_{yy}$ , and  $K_{zz}$  are the hydraulic conductivities along the x, y and z axes of the model,

which are assumed to be parallel to the principle axes of hydraulic conductivity tensor; h is the hydraulic head; Q represents the source/sink terms; and  $S_s$  is the specific storage coefficient.

(c) Unsaturated flow is one of the main processes simulated in MIKE SHE. In unsaturated areas, flow typically occurs predominantly in the vertical direction, as gravity plays a major role in the infiltration process. Therefore, unsaturated flow in MIKE SHE is calculated in a 1D vertical direction, and in this study, Richard's equation (DHI, 2023) is applied for the computation of unsaturated flow:

$$c \frac{\partial \psi}{\partial t} = \frac{\partial}{\partial z} \left( K(\theta) \frac{\partial \psi}{\partial z} \right) + \frac{\partial K(\theta)}{\partial z} - S \quad (2)$$

Where  $\psi$  is the pressure head,  $K(\theta)$  is the unsaturated hydraulic conductivity, S is the root extraction sink term and C is soil water capacity. S is calculated through transpiration in the root zone (the upper part in the unsaturated zone) for each computational node in the model. Actual transpiration is calculated in

Equation 5 below and depends on Leaf Area Index (LAI), soil moisture content in the root zone and root density.

(d) The calculation of evapotranspiration in the MIKE SHE model is based on root depth and vegetation cover density (DHI, 2023).

### 2.3.3 Multivariate linear regression analysis

Multivariate linear regression (MLR) was used to analyze the correlation between LULC changes and groundwater flow Q. The input of this model is the time-series LULC data collected from 1988 to 2022, consisting of areas of six LULC classes and the corresponding time-series Q data for the same period served as the target variable. Initial data processing involved removing any rows with missing values, leaving a final dataset of 25 years. In this 25-year dataset, the first 21 years in the duration of 1988–2018 were used as training and testing datasets with the Q generated from the MIKE SHE model. This dataset was then split into 80% for model training and 20% for testing using random sampling. Meanwhile, the last four years from 2019 to 2022 were used as a validation dataset, with the Q data being the in-situ data collected from the pilot area. An MLR model was then developed using the scikit-learn library in Python. A linear regression model was fitted to the training set to establish the relationship between the selected LULC features and groundwater flow. The trained model was then used to predict Q for a validation period of 2019–2022, based on its LULC composition. The equation of the MLR algorithm that is being fitted in the model is as follows:

$$y = \beta_0 + \beta_1X_1 + \beta_2X_2 + \beta_3X_3 + \beta_4X_4 + \beta_5X_5 + \varepsilon \quad (3)$$

where, y is Groundwater level (target variable); X1 is Bare soil (LULC feature 1); X2 is Built-up (LULC feature 2); X3 is Cropland (LULC feature 3); X4 is Forest (LULC feature 4); X5 is Rangeland (LULC feature 5); X6 is Wetland (LULC feature 6);  $\beta_0$  is Intercept term;  $\beta_1, \beta_2, \beta_3, \beta_4, \beta_5, \beta_6$  is Coefficient values corresponding to each LULC feature;  $\varepsilon$  is Error term.

### 2.3.4 Calibrations and validations

Calibrations and validations were performed on three models LULC classification model, MIKE SHE model, and MLR model.

(a) For LULC model, the results of LULC classification were evaluated using Cohen's Kappa (K) method. K is a robust statistic. It can be used to test either interrater or intrarater reliability (McHugh, 2012). K ranges from -1 to +1, with 1 indicating complete agreement between raters.

To conduct the assessment, 500 samples were

randomly selected, and distributed evenly across the six LULC classes. These samples have been made regarding Google Earth images, LULC-collected maps and field survey information. The Kappa coefficient is described by Equation 12.

$$K = (Po - Pe) / (1 - Pe) \quad (4)$$

where Po is a probability of agreement and Pe is a probability of random agreement.

(b) Calibration and validation of the MIKE SHE model for the groundwater flow are crucial processes to ensure the accuracy and reliability of the model. The MIKE SHE model for the research area in Al Ba was calibrated and validated based on measured groundwater flow data at the pilot area. During the construction of the model, many uncertainties arise, for which calibration and validation operations are important. However, due to the lack of measured groundwater flow data that can be used for calibration and validation operations, the groundwater flow simulation can only provide informative information. The study measured groundwater flow at the spring location in five phases: Phase 1 (11/2021), Phase 2 (02/2022), Phase 3 (05/2022), Phase 4 (08/2022), and Phase 5 (10/2022). Phase 1 and Phase 2 represent actual groundwater flow data during the dry season (November 2021 - March 2022), while Phase 3, Phase 4 and Phase 5 are measured during the wet season (May 2022 - October 2022). Measurements were taken at intervals of 2-3 months to ensure a suitable time gap between the actual data used for calibration and verification. The parameters and characteristics of the MIKE SHE model were adjusted to fit the observed data during the calibration step. The validation step assessed the reliability of the MIKE SHE model for the pilot watershed, using the measured data from Phase 1 and Phase 2.

(c) MLR model performance was evaluated on both training and test sets using metrics including R<sup>2</sup>, MAE, MSE, and RMSE to check for overfitting. According to Chicco et al., (2021), the R<sup>2</sup> (Coefficient of determination) metric (Equation 13) reveals the proportion of the dependent variable's (y) variability attributed to the independent variables X. Its scale ranges between 0 and 1, with a score nearer to 1 reflecting a stronger association. The MAE (Mean Absolute Error) is the average over the test sample of the absolute differences between prediction and actual observation (Equation 14). The MSE (Mean Squared Error) represents the average squared deviation between estimated values and the actual values (Chicco et al., 2021). Its square root is known as the RMSE (Root Mean Squared Error) which has the same units as the variable. Both MSE and RMSE take the error magnitude into account (Equations 15

and 16).

$$R^2 = 1 - (SS_{res}/SS_{tot}) \quad (5)$$

$$MAE = \frac{1}{n} \sum_{i=1}^n |y_i^{real} - y_i^{pred}| \quad (6)$$

$$MSE = \frac{1}{n} \sum_{i=1}^n (y_i^{real} - y_i^{pred})^2 \quad (7)$$

$$RMSE = \sqrt{MSE} \quad (8)$$

where  $SS_{res}$  is the Residual sum of squares;  $SS_{tot}$  is the Total sum of squares;  $y_i^{real}$  is observations;  $y_i^{pred}$  is predictions.

### 3. RESULTS AND DISCUSSION

#### 3.1. LULC situation from 1988 to 2022

The Kappa (K) results for 25 years of LULC categorization vary from 0.844 to 0.898, with an average of 0.871. These results show that the LULC classifications for Al Ba's pilot area are suitable for use as input data for the MIKE SHE model and subsequent related LULC analysis.

Between 1988 and 2022, the land cover in the study area underwent significant changes. Local authorities in Al Ba Commune and Chu Se District identified population growth, forest resource encroachment, and agricultural expansion as the main drivers of forest degradation. Reforestation efforts are often ineffective due to the remoteness of areas, limited resources for investment among local families, and reliance on inconsistent provincial funding. This results in small and dispersed afforested patches. In addition, recurrent droughts leading to forest fires and poor soil nutrients contribute to the loss of forested areas.

Based on Figure 6, spatially, the bare soil class was initially central from 1988-1992, then spread eastward, dominating by 2001-2022, and replacing forests. Cropland and built-up areas retook central bare soil from 2014 to 2021. Urban areas, starting in the center from 1988 to 1990, expanded westward and south/east from 1992 to 2006, covering the entire study area by 2010 to 2022. Croplands centered initially, expanded westward until 2006, and then replaced bare land and forests eastward until 2022. Forests covered east and west in 1988, but the western forest declined from 1989, while eastern forests disappeared from 2020, with slight rebounds in 2006 and 2020. By 2022, scarce forest remained in the northeast. Rangelands and wetlands fluctuated seasonally, with no clear trends.

The analysis of LULC trends (see Figure 7) reveals a decrease in natural land covers, such as forests and rangelands, in contrast to the expansion of anthropogenic land covers, including croplands, built-up areas, and bare lands. In 1988, forested areas were the most extensive at 24.83 km<sup>2</sup>, while cropland

(5.11 km<sup>2</sup>) and rangeland (4.66 km<sup>2</sup>) were less extensive. Over the years, the built-up area has increased more than sixfold to 3.05 km<sup>2</sup> in 2022, and bare soil has more than doubled to 5.26 km<sup>2</sup>. These changes are indicative of escalating urbanization and land degradation.

The breakdown by decade illustrates the dynamic changes in LULC. Between 1988 and 1997, the main driver of change was agricultural expansion, with cropland area increasing to 6.39 km<sup>2</sup> and built-up area doubling to 0.93 km<sup>2</sup>. Forests and rangelands experienced only slight decreases. Between 1998 and 2006, crop cultivation intensified, peaking at 17.4 km<sup>2</sup>, while forest coverage decreased to 7.59 km<sup>2</sup> and built-up areas and rangelands showed fluctuations. Between 2008 and 2017, there was a critical period where crop cultivation stabilized at around 17.3 km<sup>2</sup>, bare soil increased to 7.73 km<sup>2</sup>, and forests reached a low point of 2.84 km<sup>2</sup> in 2015, indicating severe degradation. Urban areas continued to expand steadily. Between 2018 and 2022, there were variations in LULC distribution, with bare soil areas peaking at 6.30 km<sup>2</sup> in 2019, followed by a decline and then an increase to 5.26 km<sup>2</sup> in 2022. Built-up areas consistently grew, reflecting ongoing urbanization. Wetlands experienced dramatic fluctuations, peaking at 6.56 km<sup>2</sup> in 2019 before declining and then moderately increasing to 2.53 km<sup>2</sup> in 2022. The area of cropland decreased significantly, and the forest cover exhibited a pattern of initial decline, followed by a slight increase in 2020, and then another decrease to 8.60 km<sup>2</sup> in 2022, demonstrating the changing dynamics in forestry. The rangeland increases from 9.07 km<sup>2</sup> to 13.15 km<sup>2</sup>, indicating a shift towards grazing.

During 2019-2020, the forest area in Chu Se district increased. Local authorities' records indicate that the main forest type in the area is acacia, which is mainly cultivated for production rather than conservation purposes. In 2019, Chu Se District reported a total forest area of 120.98 km<sup>2</sup>, with 2.06 km<sup>2</sup> allocated to timber production. Out of the total area, only 0.29 km<sup>2</sup> were officially designated as forest, while 1.77 km<sup>2</sup> had not yet become forests. By 2020, the area allocated to timber production had increased slightly to 1.95 km<sup>2</sup>. As a result of this situation, there has been a modest increase in forest cover within Al Ba commune. Overall, the analysis indicates a reduction in forest area in favor of expanding agriculture and urbanization.

#### 3.2 Groundwater flow simulation

The calibration and validation of the model demonstrate a comparison between the modelled and measured groundwater flow data at the spring location

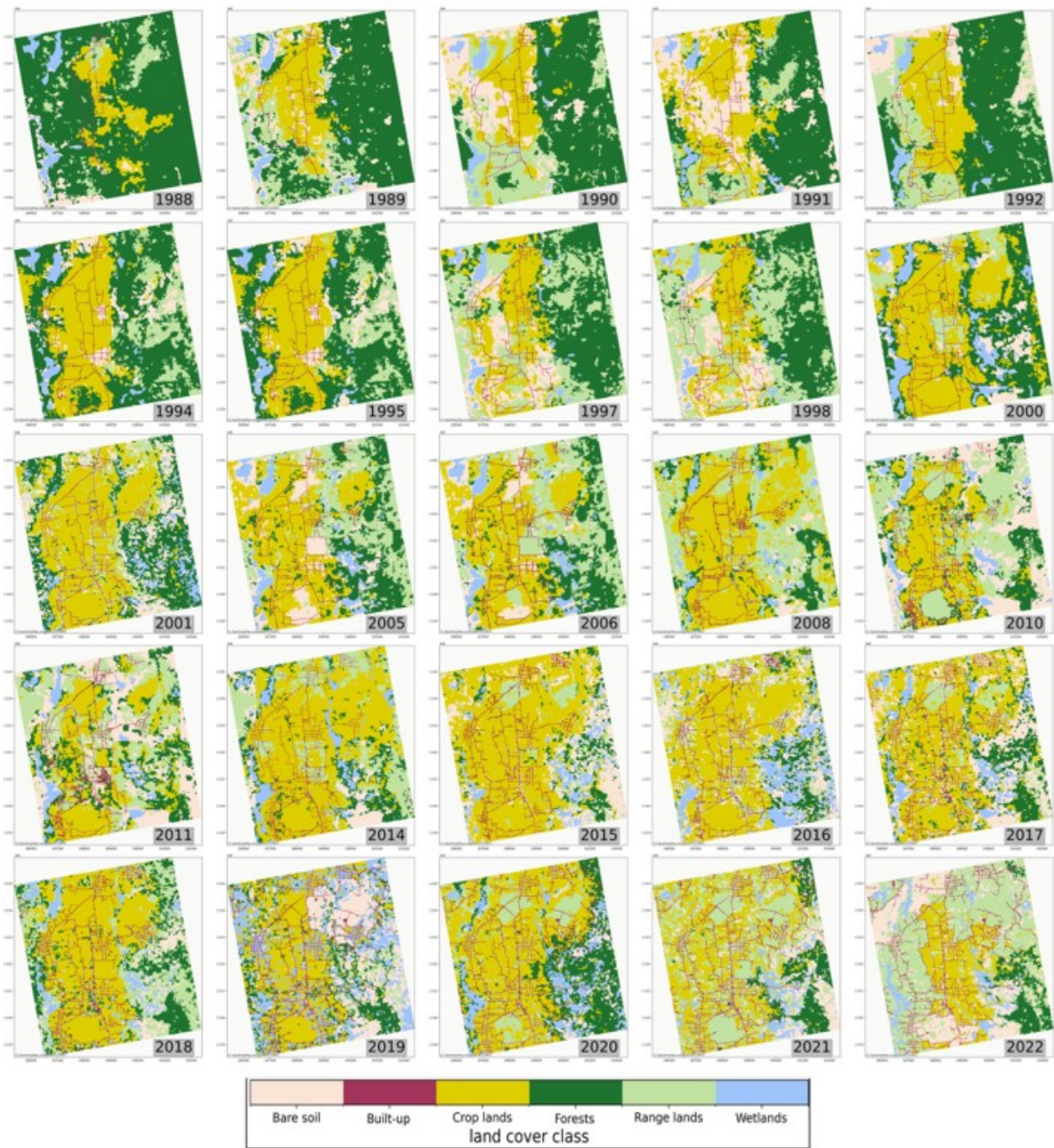


Figure 6. LULC maps of Al Ba's pilot area from 1988 to 2022

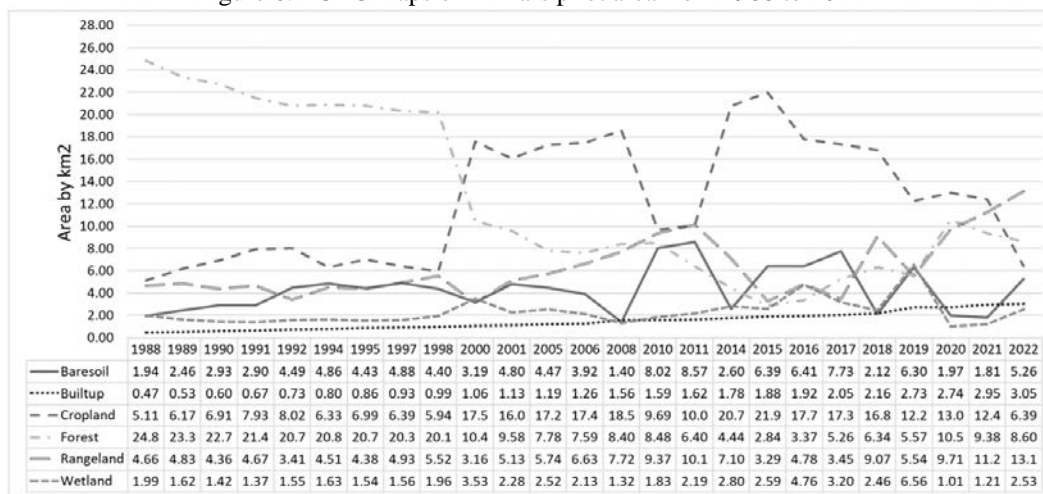


Figure 7. Statistics on changes in LULC area from 1988 to 2022

(Figure 8). Despite the limitations in sampling data from the pilot basin, the model has undergone necessary adjustments to make the model data align with the measured data in Phase 3, 4, and 5. Moreover, the validation results of the model with the measured data from Phases 1 and 2 have shown the model's suitability for the pilot basin in simulating groundwater flow. The study involved simulating a groundwater model in the Al Ba area of Gia Lai province over a period of 25 years, from 1988 to 2022.

Figure 9 shows the average annual groundwater flow from 1988-2022. Overall, there has been a 5.8% decrease in flow rate from 1988 (0.69 l/s) to 2022 (0.65 l/s). The highest average flow rate was recorded in 1992 at 0.69 l/s, while the lowest was recorded in 2016 at 0.598 l/s.

Over 34 years, the Gia Lai-Central Highlands experienced seven major droughts during dry seasons, specifically in 1988-1990, 1993-1996, 1998-2003, 2008-2011, 2014-2016, and 2018-2019 (Le & Nguyen, 2005; Nguyen, 2011; Bui, 2014; Cao et al., 2016; Tuan, 2016; Tran, 2019). These droughts were linked to an early cessation of the rainy season, resulting in lower-than-average rainfall and underfilled water reservoirs, some reaching as low as 20-30% capacity (Bui, 2014). The region faced insufficient water flow, droughts, and shortages exacerbated by increased water demand for agriculture exceeding irrigation capacity (Le & Nguyen, 2005; Bui, 2014). The Central Highlands' water supply relies on rain, soil water retention, and vegetation, and water regulation by hydroelectric reservoirs has further stressed agricultural water intake, impeding efforts to restore natural downstream flows during droughts (Bui, 2014;

Tran, 2019). These droughts have caused economic, social, and environmental damages, including heightened forest fire risks and water scarcity for ecosystems. Conversely, periods of increased groundwater flow occurred in 2012-2013, 2016-2018, and 2020-2021, often due to floods and storms (Le, 2013; Nguyen, 2014; Gia Lai People Committee, 2017; VMHA, 2020; Kieu & Le, 2021). Hydroelectric projects have also contributed to unpredictable Ba River flows by releasing floodwaters during the rainy season, causing extensive flooding (Nguyen, 2014).

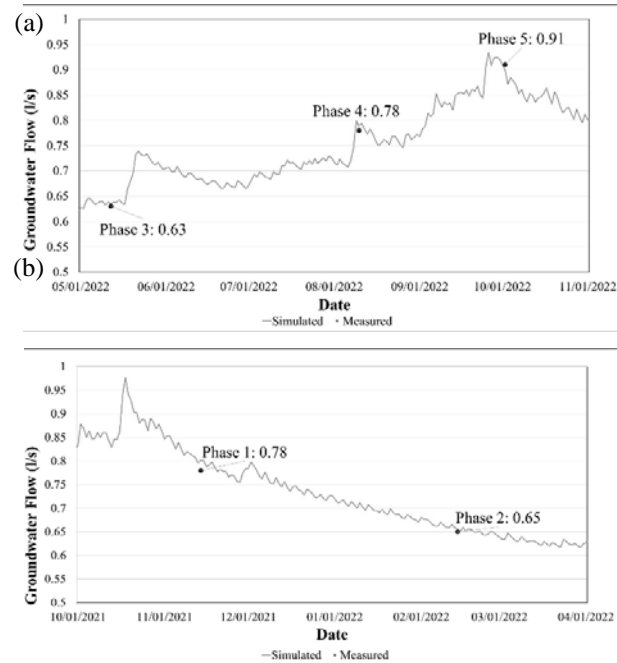


Figure 8. (a) Calibration results and (b) Validation results of MIKE SHE model

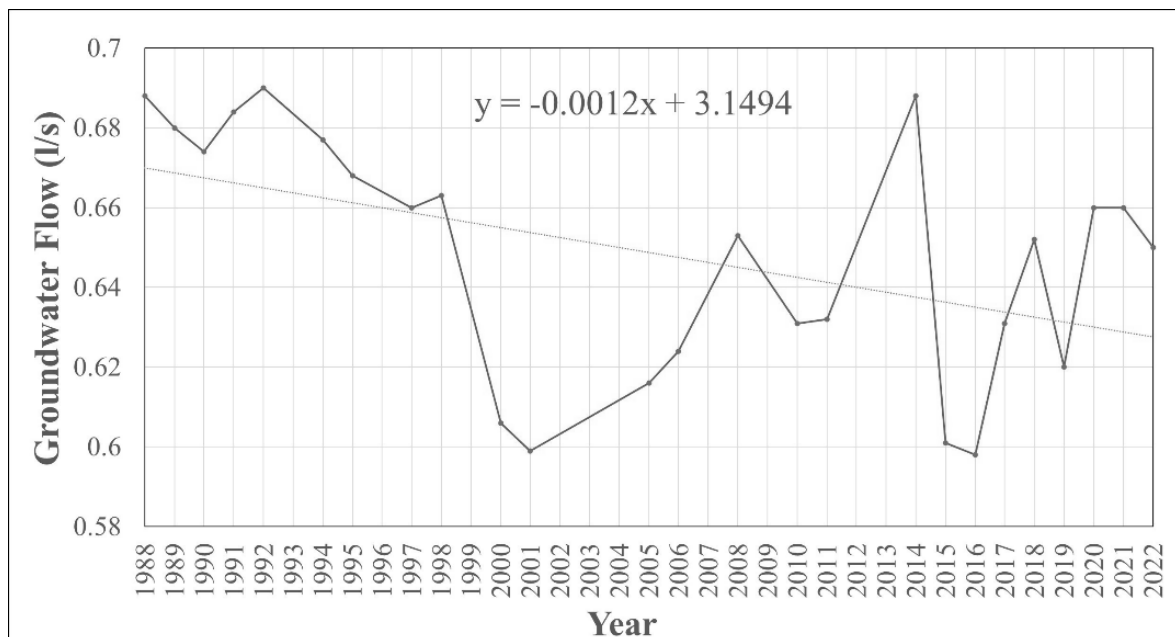


Figure 9. Average annual groundwater flow simulated from the MIKE SHE model

### 3.3 The correlation between groundwater flow and LULC changes

According to Table 3 and Figure 10. The MLR model, which was developed using Python, accurately predicts the relationship between LULC changes and groundwater flow (Q). The model has a training R<sup>2</sup> value of 0.914 and a prediction R<sup>2</sup> value of 0.912. Its predictive performance on withheld data is outstanding, with an R<sup>2</sup> value of 0.808 and low errors. Validation on data from 2019-2022 yielded an R<sup>2</sup> of 0.832, confirming its efficacy in capturing the effects of shifting LULC patterns on groundwater flow. The model's dependable generalization potential is evident in the regression analysis results.

However, the positive coefficients of LULC classes mentioned in Table 3 from the MLR model contradicted the hypothesis that an increase in built-up, bare soil, and agricultural lands leads to a decrease in groundwater recharge. To examine this in more detail, we calculated the coefficients between each LULC class and Q. As shown in Figure 11, there is a clear relationship between each LULC class and Q. Bare soil, built-up areas, cropland, and wetlands have negative coefficients of -0.0058, -0.01289, -0.0034, and -0.01235, respectively. On the other hand, forest (0.0025) and rangeland (0.00076) show a positive trend with Q. These findings led to the hypothesis that multicollinearity, a statistical concept where two or more independent variables display significant correlation. Multicollinearity can increase the variance of the estimated regression coefficients, making it difficult to isolate the impact of individual LULC classes on Q.

To address this, we used the Variance Inflation Factor (VIF), as shown in equation 17, to measure the extent of multicollinearity. High VIF values would confirm the presence of multicollinearity in the model, which could explain the unexpected positive coefficients for certain LULC classes. Accurately interpreting how land use and land cover changes affect groundwater recharge is crucial for refining the model.

$$VIF_i = \frac{1}{1-R_i^2} \quad (9)$$

where R<sub>i</sub><sup>2</sup> is the coefficient of determination of regression of an independent variable against all other variables.

Table 2 shows that the VIF results show a strong correlation among land use types with a high level of multicollinearity, with the highest value being 10.34 (built-up class). This affects the interpretability of a regression model that includes these variables, as it would be difficult to isolate the effect of any one variable on the dependent variable

(Q). The presence of multicollinearity in the data could be attributed to the fact that these land use types are derived from the same geographical area. It is logical to assume that they would display a high correlation since a decrease in one type might lead to an increase in others to compensate. This phenomenon results in multicollinearity.

Table 2. VIF results

No.	LULC class	R <sup>2</sup>	VIF
1	Bare soil	0.88	8.56
2	Built-up	0.90	10.34
3	Cropland	0.89	9.47
4	Forest	0.74	3.88
5	Rangeland	0.87	7.51
6	Wetland	0.86	6.95

To address multicollinearity, LULC classes were combined (James et al., 2013; Harrell, 2015). and ridge regression (Hoerl & Kennard, 1970; Kidwell & Brown, 1982; Bager et al., 2017) was used.

Specifically, non-vegetation classes (bare soil, built-up, and wetland) were grouped, The remaining classifications were retained to represent the various types of vegetation cover (cropland, forest, rangeland). Therefore, the number of LULC classes has been reduced to four categories: non-vegetation, cropland, forest, and rangeland.

New LULC classes were used as independent variables in a ridge regression to analyze Q, addressing multicollinearity, which inflates variances in the least squares estimates (Hoerl & Kennard, 1970; Kidwell & Brown, 1982; Bager et al., 2017). Ridge regression corrects this by adding a bias factor, alpha, to reduce overfitting (Bager et al., 2017). Alpha was optimized using K-Fold cross-validation within a range of 1 to 100, selecting the one minimizing MSE on the validation set (Scikit-learn, 2023). The model was trained on an 80% and tested 20% random subset of data from 1988-2018, and validated with 2019-2022 in-situ data.

Table 4 and Figure 12 displays the ridge regression model's results, indicating the relationship between LULC classes and groundwater flow (Q). The optimal alpha for the model was set at 74, fine-tuning its complexity (Scikit-learn, 2023). Performance metrics for the model on the training set included an R<sup>2</sup> of 0.908, MSE of 6.48e<sup>-05</sup>, and MAE of 0.0167, while the test set showed similar R<sup>2</sup>, MSE, and MAE values of 0.904, 6.77e<sup>-05</sup>, and 0.0069, respectively For the forecasting module, the model attained an R<sup>2</sup> score of 0.877, an MSE of 0.00524, and an MAE of 3.30e<sup>-05</sup>. These results imply that the model displays a high degree of predictive precision, accounting for roughly 87.7% of the variation in

groundwater movement for in-situ data.

The ridge regression model's coefficients for non-vegetation and cropland were negative (-0.00211 and -0.00058), suggesting these classes decrease groundwater flow, possibly due to reduced infiltration (Wakode et al., 2018; Siddik et al., 2022b). This may be attributed to various factors, such as irrigating practices that decrease the amount of water penetrating the ground, or the cultivation of certain crops that diminish the soil's permeability (Foster et al., 2018; Mukherjee et al., 2022). In contrast, forest and rangeland had positive coefficients (0.00192 and 0.001176), implying their increase leads to more groundwater flow, attributable to better water infiltration and storage (Ilstedt et al., 2016; Onyango et al., 2016; Owuor et al., 2016; Wilcox et al., 2017; Shannon et al., 2019; Zhang et al., 2023). Thus, the final regression equation for Q prediction from LULC areas is expressed as Equation 18.

$$Q_{pred} = -0.64785 - 0.0021 \times X1 - 0.00058 \times X2 + 0.00192 \times X3 + 0.001176 \times X4 \quad (10)$$

where  $Q_{pred}$  is predicted groundwater flow. X1 is Non-vegetation (LULC feature 1); X2 is Cropland (LULC feature 2); X3 is Forest (LULC feature 3); X4 is Rangeland (LULC feature 4).

The coefficient for each LULC class has a small decimal compared to the intercepts (-0.64), which can be interpreted in several ways. Firstly, the areas of LULC classes are likely measured in large units, and even small changes in these units can

represent substantial physical areas. Secondly, as a ridge regression model, it is designed to handle multicollinearity among predictors by imposing a penalty on the size of the coefficients. This can shrink the coefficients towards zero, particularly if the model is trying to manage overfitting or if the predictors are highly correlated. Lastly, the small coefficients indicate that the contribution of each LULC class to the variation in groundwater flow is less significant than the baseline flow determined by the intercept, which may be heavily influenced by other factors such as climate, soil properties, topography, or other hydrological factors not captured by LULC alone.

In summary, the merging of LULC classes and the application of ridge regression have provided a viable approach to address the issue of multicollinearity and assist in understanding the relationship between land use patterns and groundwater flow.

#### 4. CONCLUSIONS

This study applied a process-based hydrological modelling and integrated remote sensing methodology to measure the correlations between changes in LULC and groundwater flow trends in the Al Ba pilot region of Gia Lai Province, Vietnam, over the period 1988-2022. High-resolution satellite imagery from the LST5, LST8 and S2A missions was used to generate detailed LULC

Table 3. Evaluations of MLR results

Evaluations for training model:		Evaluations for prediction model:			
R <sup>2</sup> score	0.914	R <sup>2</sup> score	0.912	Class	Coefficient
Intercept	-4.534	Intercept	-4.565	Bare soil	0.129
Evaluations of the testing model:		Validation for prediction model:		Built-up	0.177
R <sup>2</sup> score	0.808	R <sup>2</sup> score	0.832	Cropland	0.131
MAE	0.013	MAE	0.007	Forest	0.136
MSE	0.0002	MSE	8.51E-05	Rangeland	0.132
RMSE	0.014	RMSE	0.009	Wetland	0.121

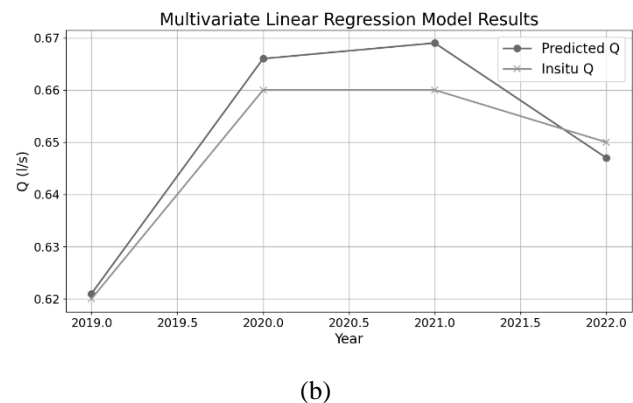
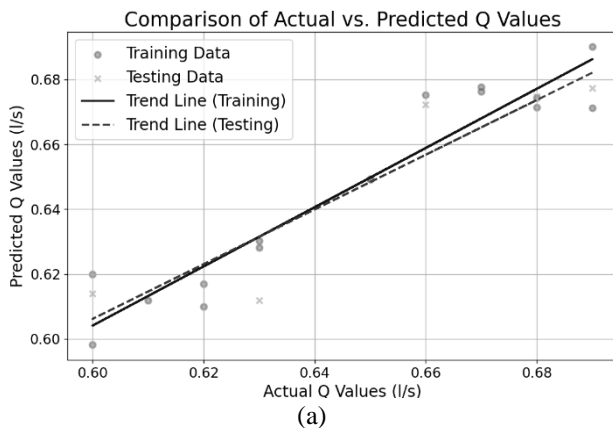


Figure 10. (a) Performance of training and testing models; (b) Performance of prediction models of MLR

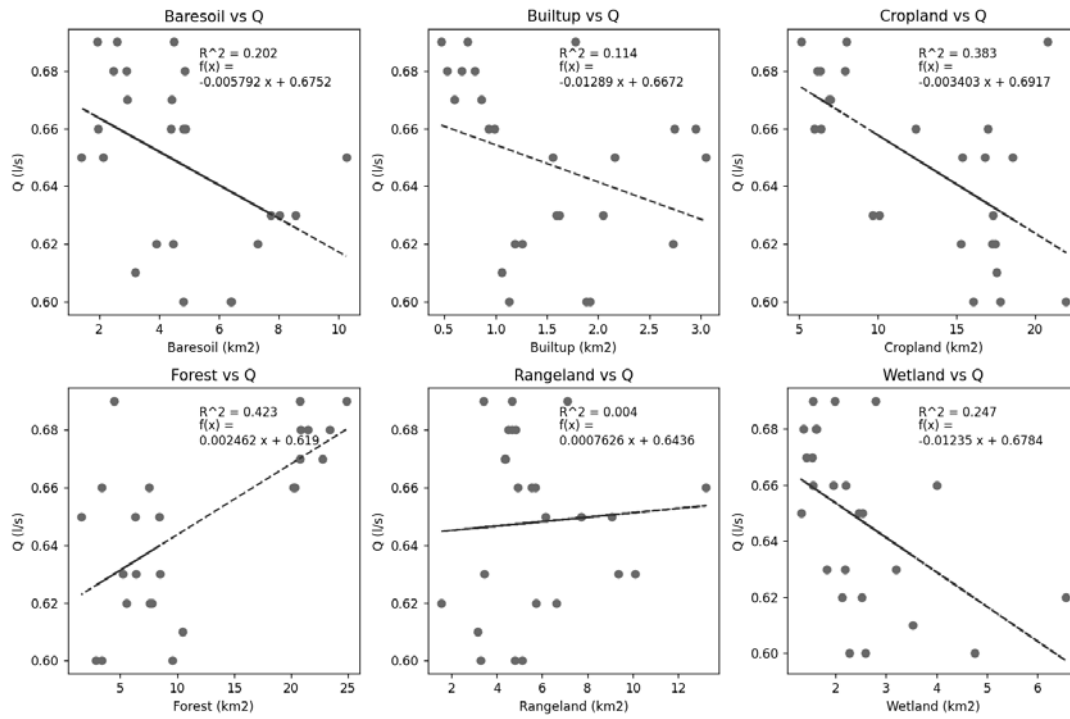
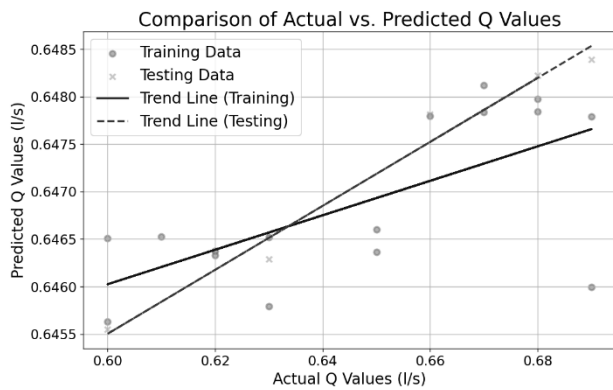


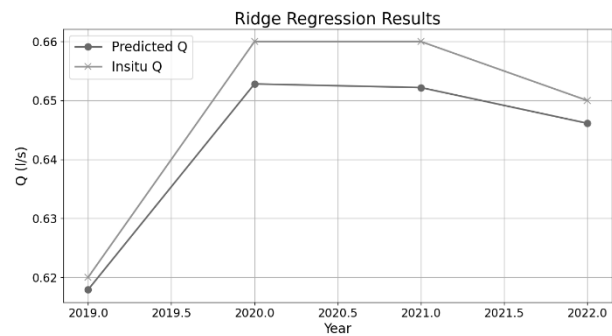
Figure 11. Correlation between each LULC class and groundwater flow Q

Table 4. Evaluation of Ridge Regression Results

Model	R <sup>2</sup> score	MAE	MSE
Train model	0.908	6.48E-05	1.67E-02
Test model	0.904	6.77E-05	0.006936
Prediction model	0.877	0.005236	3.30E-05
LULC class	Coefficient	LULC class	Coefficient
Non-vegetation	-0.00211	Rangeland	0.001176
Cropland	-0.00058	Intercept	0.640785
Forest	0.00192	<b>Best alpha</b>	<b>74</b>



(a)



(b)

Figure 12. (a) Performance of training and testing models; (b) Performance of prediction models of ridge regression

maps. The maps depict changes in LULC that have occurred over the years, including a decrease in forest cover and an increase in bare soil, cropland and urban infrastructure. The MIKE SHE hydrological model was developed to simulate historical groundwater flow trends. However, the calibration and validation of the model were limited due to the limited availability of measured groundwater flow data.

The study then analysed the effects of LULC changes on groundwater flow using the MLR model. Despite the high R<sup>2</sup> scores obtained by the MLR model for both training and prediction, it indicated a positive correlation between LULC classes and groundwater flow, which contradicts previous findings. These anomalies in the MLR results led to the identification of multicollinearity problems among the LULC

variables, evidenced by VIF values exceeding the accepted threshold.

To address these issues, we employed grouping method and ridge regression model. This involved combining certain LULC classes into a 'non-vegetation' category and introducing a bias factor, alpha, to manage variance. Cross-validation was used to identify the optimal alpha that corrected the coefficients of the MLR. This revealed a more intricate relationship, where non-vegetative cover, such as urban and bare soil, had a negative impact on groundwater flow, while vegetation, such as forests and rangeland, had a positive impact. The Ridge Regression analysis provided a refined perspective on the effects of LULC on groundwater and proved to be an essential tool for strategic environmental management and conservation efforts.

In conclusion, this comprehensive analysis, which incorporates both remote sensing and process-driven hydrological modeling, confirms the significant cumulative effects of human-induced LULC in altering the recharge and flow processes of groundwater systems. It is crucial to evaluate these dynamic LULC impacts, which act as a significant non-point source that determines the sustainability of aquifers to regulate the use of aquifers in the Central Highlands region under varying environmental conditions. Hence, establishing efficient groundwater management tactics necessitates a clear understanding of LULC's causal connections and its impact on the aquifer.

### Acknowledgments

We would like to express our deep gratitude to the institutions and local authorities involved for their invaluable assistance in completing this study.

First and foremost, we acknowledge the financial support provided for this study under project code DTDL.CN-67/21, which was carefully managed by the Vietnam Academy for Water Resources.

Our sincere thanks go to the executing agency, the Southern Institute of Water Resources Research, whose dedication and expertise were fundamental in advancing the research objectives.

We are particularly grateful to the local authorities of Al Ba Commune, Chu Se District, Gia Lai Province. Their cooperation was essential in facilitating our fieldwork, providing access to critical documents, and providing local insights that were crucial to the integrity of our research findings.

### REFERENCES

- Ahmad, W., Iqbal, J., Nasir, M. J., Ahmad, B., Khan, M. T., Khan, S. N., & Adnan, S., 2021. *Impact of land use/land cover changes on water quality and human health in district Peshawar Pakistan*. Scientific Reports 2021 11:1, 11(1), 1–14. <https://doi.org/10.1038/s41598-021-96075-3>
- Al-Kindi, K. M., Alqurashi, A. F., Al-Ghafri, A., & Power, D., 2023. *Assessing the Impact of Land Use and Land Cover Changes on Aflaj Systems over a 36-Year Period*, Remote Sensing 2023, Vol. 15, Page 1787, 15(7), 1787. <https://doi.org/10.3390/RS15071787>
- Ansari, T. A., Katpatal, Y. B., & Vasudeo, A. D., 2016. *Spatial evaluation of impacts of increase in impervious surface area on SCS-CN and runoff in Nagpur urban watersheds, India*, Arabian Journal of Geosciences, 9(18), 1–15. <https://doi.org/10.1007/S12517-016-2702-5/METRICS>
- Bager, A., Roman, M., Algelidh, M., & Mohammed, B., 2017. *Addressing multicollinearity in regression models: a ridge regression application*, MPRA - Munich Personal RePEc Archive, 81390.
- Baker, T. J., & Miller, S. N., 2013. *Using the Soil and Water Assessment Tool (SWAT) to assess land use impact on water resources in an East African watershed*, Journal of Hydrology, 486, 100–111. <https://doi.org/10.1016/J.JHYDROL.2013.01.041>
- Bouillet, J. P., Bordron, B., Laclau, J. P., Robin, A., Gonçalves, J. L. M., Abreu-Junior, C. H., Trivelin, P. C. O., Nouvellon, Y., & le Maire, G., 2023. *Early and long-distance uptake by Eucalyptus grandis of N, K and Ca tracers injected down to a depth of 7 m*, Forest Ecology and Management, 550, 121507. <https://doi.org/10.1016/J.FORECO.2023.121507>
- Bui, D. L., 2014. *Drought situation in recent years and assessment of the dry season drought situation in 2014*, Vietnam Journal of Hydro-Meteorology, 4, 1–7, (in Vietnamese).
- Cao, N., Dinh, T., & Hoang, T., 2016. *Abnormalities in the Central Highlands*, Nguoi Lao Dong. <https://nld.com.vn/thoi-su-trong-nuoc/bat-thuong-tay-nguyen-20160904213345488.htm> (in Vietnamese).
- Chicco, D., Warrens, M. J., & Jurman, G., 2021. *The coefficient of determination R-squared is more informative than SMAPE, MAE, MAPE, MSE and RMSE in regression analysis evaluation*, PeerJ Computer Science, 7, 1–24. <https://doi.org/10.7717/PEERJ-CS.623/SUPP-1>
- Dan, M., 2016. *Groundwater exploitation in the Central Highlands still has many shortcomings*, Tai Nguyen va Moi Truong. <https://baotainguyenmoitruong.vn/khai-thac-nuoc-ngam-o-tay-nguyen-con-nhieu-bat-cap-235320.html> (in Vietnamese).
- Devi, A. B. V., Nair, A. M., Devi, A. B. V., & Nair, A. M., 2020. *Evaluation of the impact of Long-term Land Use Land Cover Change on Groundwater Recharge in the Periyar River Watershed, India*, AGUFM, 2020, GC056-0004. <https://ui.adsabs.harvard.edu/abs/2020AGUFMGC0560004D/abstract>
- DHI, 2023. *User Guide and Reference Manual*. In DHI (Vol.

- 11).
- Duranel, A., Thompson, J. R., Burningham, H., Durepaire, P., Garambois, S. phane, Wyns, R., & Cubizolle, H.,** 2021. *Modelling the hydrological interactions between a fissured granite aquifer and a valley mire in the Massif Central, France*, Hydrology and Earth System Sciences, 25(1), 291–319. <https://doi.org/10.5194/hess-25-291-2021>
- DWRM,** 2015. *Central Highlands: Declining groundwater resources*. Department of Water Resources Management. <http://dwr.gov.vn/index.php?language=vi&nv=news&op=Tai-nguyen-nuoc/Tay-Nguyen-Suy-giam-nguo-n-nuoc-ngam-4587> (in Vietnamese)
- El-Khoury, G.,** 2022. *Land Use, Land Cover Changes and the link with groundwater*, In Governance in NAHR AL-JAOUZ river basin, Lebanon.
- Elmahdy, S., Mohamed, M., & Ali, T.,** 2020. *Land Use/Land Cover Changes Impact on Groundwater Level and Quality in the Northern Part of the United Arab Emirates*, Remote Sensing 2020, Vol. 12, Page 1715, 12(11), 1715, <https://doi.org/10.3390/RS12111715>
- ESRI,** 2023. *Classify Objects Using Deep Learning (Image Analyst)*. ArcGIS Pro | Documentation. <https://pro.arcgis.com/en/pro-app/latest/tool-reference/image-analyst/classify-objects-using-deep-learning.htm>
- Fienen, M. N., & Arshad, M.,** 2016. *The international scale of the groundwater issue*. Integrated Groundwater Management: Concepts, Approaches and Challenges, 21–48. [https://doi.org/10.1007/978-3-319-23576-9\\_2/FIGURES/1](https://doi.org/10.1007/978-3-319-23576-9_2/FIGURES/1)
- Foster, S., Pulido-Bosch, A., Vallejos, Á., Molina, L., Llop, A., & MacDonald, A. M.,** 2018. *Impact of irrigated agriculture on groundwater-recharge salinity: a major sustainability concern in semi-arid regions*, Hydrogeology Journal, 26(8), 2781–2791. <https://doi.org/10.1007/S10040-018-1830-2/FIGURES/7>
- Gia Lai People Committee,** 2017. *Decision - promulgating the 2017 natural disaster prevention plan in Gia Lai province (502/QĐ-UBND)* (in Vietnamese)
- González-Trinidad, J., A., H. E., Pacheco-Guerrero, Olmos-Trujillo, & Bautista-Capetillo, E.,** 2017. *Dynamics of land cover changes and delineation of groundwater recharge potential sites*. Applied Ecology and Environmental Research, 15(3), 387–402. [https://doi.org/10.15666/aeer/1503\\_387402](https://doi.org/10.15666/aeer/1503_387402)
- Han, D., Currell, M. J., Cao, G., & Hall, B.,** 2017. *Alterations to groundwater recharge due to anthropogenic landscape change*, Journal of Hydrology, 554, 545–557, <https://doi.org/10.1016/J.JHYDROL.2017.09.018>
- Harrell, F. E.,** 2015. *Regression Modeling Strategies With Applications to Linear Models, Logistic and Ordinal Regression, and Survival Analysis (Second)*. Springer Series in Statistics. <http://www.springer.com/series/692>
- Hoerl, A. E., & Kennard, R. W.,** 1970. *Ridge Regression: Biased Estimation for Nonorthogonal Problems*, Technometrics, 12(1), 55–67. <https://doi.org/10.1080/00401706.1970.10488634>
- Huang, Z., Yuan, X., Sun, S., Leng, G., & Tang, Q.,** 2023. *Groundwater Depletion Rate Over China During 1965–2016: The Long-Term Trend and Inter-annual Variation*, Journal of Geophysical Research: Atmospheres, 128(11), e2022JD038109. <https://doi.org/10.1029/2022JD038109>
- Hussain, Z.,** 2022. *Explained: Excessive Groundwater Extraction Leading To Fall In Water Levels & Why It's Not Good*. Exolainers. <https://www.indiatimes.com/explainers/news/excessive-groundwater-extraction-leading-to-fall-in-water-levels-explainer-568919.html>
- Istedt, U., Bargués Tobella, A., Bazié, H. R., Bayala, J., Verbeeten, E., Nyberg, G., Sanou, J., Benegas, L., Murdiyarso, D., Laudon, H., Sheil, D., & Malmer, A.,** 2016. *Intermediate tree cover can maximize groundwater recharge in the seasonally dry tropics*, Scientific Reports 2016 6:1, 6(1), 1–12. <https://doi.org/10.1038/srep21930>
- Im, S., Kim, H., Kim, C., & Jang, C.,** 2009. *Assessing the impacts of land use changes on watershed hydrology using MIKE SHE*, Environmental Geology, 57(1), 231–239. <https://doi.org/10.1007/S00254-008-1303-3>
- James, G., Witten, D., Hastie, T., & Tibshirani, R.,** 2013. *An Introduction to Statistical Learning*, Springer Texts in Statistics. <http://www.springer.com/series/417>
- Keilholz, P., Disse, M., & Halik, Ü.,** 2015. *Effects of land use and climate change on groundwater and ecosystems at the middle reaches of the Tarim River using the MIKE SHE integrated hydrological model*, Water (Switzerland), 7(6), 3040–3056. <https://doi.org/10.3390/w7063040>
- Kidwell, J. S., & Brown, L. H.,** 1982. *Ridge Regression as a Technique for Analyzing Models with Multicollinearity*, Journal of Marriage and the Family, 44(2), 287. <https://doi.org/10.2307/351539>
- Kieu, P., & Le, N.,** 2021. *Many localities suffered damage due to floods, Gia Lai Provincial People's Committee directed urgent response to natural disasters*, Gia Lai Online. <https://baogialai.com.vn/nhieu-dia-phuong-thiet-hai-do-mua-lu-ubnd-tinh-gia-lai-chi-dao-khan-truong-ung-pho-voi-thien-tai-post158076.html>
- Koshy, J.,** 2023. *Groundwater exploitation is silently sinking the ground beneath India's feet - The Hindu*. The Hindu. <https://www.thehindu.com/sci-tech/energy-and-environment/groundwater-exploitation-is-silently-sinking-the-ground-beneath-indias-feet/article66847379.ece>
- Kuroda, K., Hayashi, T., Do, A. T., Canh, V. D., Nga, T. T. V., Funabiki, A., & Takizawa, S.,** 2017. *Recharge des eaux souterraines dans des régions suburbaines de Hanoi, Vietnam: effet de la diminution des niveaux des masses d'eaux de surface et des changements d'occupation du sol*, Hydrogeology Journal, 25(3), 727–742. <https://doi.org/10.1007/S10040-016-1528->

- Lancia, M., Yao, Y., Andrews, C. B., Wang, X., Kuang, X., Ni, J., Gorelick, S. M., Scanlon, B. R., Wang, Y., & Zheng, C., 2022.** *The China groundwater crisis: A mechanistic analysis with implications for global sustainability*, *Sustainable Horizons*, 4, 100042.  
<https://doi.org/10.1016/J.HORIZ.2022.100042>
- Le, B. H., & Nguyen, Q. H., 2005.** *Situation of drought, water shortage and orientation of prevention solutions from the perspective of water resources management*, *Vietnam Journal of Hydro-Meteorology*, 538(10), 9–18. (in Vietnamese)
- Le, H., 2013.** *During the 2013 rainy season, many unusual developments occurred*. Gia Lai Online. <https://m.baogialai.com.vn/mua-mua-lu-nam-2013-nhieu-dien-bien-bat-thuong-post150408.amp> (in Vietnamese)
- Lymburner, L., Beggs, P. J., & Jacobson, C. R., 2000.** *Estimation of canopy-average surface-specific leaf area using Landsat TM data*, *Photogrammetric Engineering and Remote Sensing*, 66(2), 183–191.
- Ma, L., He, C., Bian, H., & Sheng, L., 2016.** *MIKE SHE modeling of ecohydrological processes: Merits, applications, and challenges*, *Ecological Engineering*, 96, 137–149.  
<https://doi.org/10.1016/J.ECOLENG.2016.01.008>
- McHugh, M. L., 2012.** *Interrater reliability: the kappa statistic*, *Biochemia Medica*, 22(3), 276.  
<https://doi.org/10.11613/bm.2012.031>
- Mensah, J. K., Ofosu, E. A., Yidana, S. M., Akpoti, K., & Kabo-bah, A. T., 2022.** *Integrated modeling of hydrological processes and groundwater recharge based on land use land cover, and climate changes: A systematic review*, *Environmental Advances*, 8.  
<https://doi.org/10.1016/J.ENVADV.2022.100224>
- MIKE SHE, 2023.** *Fully integrated hydrological modelling*. [www.Mikepoweredbydhi.Com](http://www.mikepoweredbydhi.com).  
<https://www.mikepoweredbydhi.com/products/mike-she>
- Mojid, M. A., & Mainuddin, M., 2021.** *Water-Saving Agricultural Technologies: Regional Hydrology Outcomes and Knowledge Gaps in the Eastern Gangetic Plains—A Review*, *Water* 2021, Vol. 13, Page 636, 13(5), 636.  
<https://doi.org/10.3390/W13050636>
- Mondal, K. C., Rathod, K. G., Joshi, H. M., Mandal, H. S., Khan, R., Rajendra, K., Mawale, Y. K., Priya, K., & Jhariya, D. C., 2020.** *Impact of Land-use and Land-cover Change on Groundwater Quality and Quantity in the Raipur, Chhattisgarh, India: A Remote Sensing and GIS approach*, *IOP Conference Series: Earth and Environmental Science*, 597(1), 012011.  
<https://doi.org/10.1088/1755-1315/597/1/012011>
- Mukherjee, I., Singh, U. K., & Chakma, S., 2022.** *Evaluation of groundwater quality for irrigation water supply using multi-criteria decision-making techniques and GIS in an agro-economic tract of Lower Ganga basin, India*, *Journal of Environmental Management*, 309, 114691.  
<https://doi.org/10.1016/J.JENVMAN.2022.114691>
- Nguyen, D. H., 2011.** *Drought and water security in the Central Highlands*. *Vietnam Association for Conservation of Nature and Environment*. <http://vacne.org.vn/han-han-va-an-ninh-nuoc-tai-tay-nguyen/25383.html> (in Vietnamese)
- Nguyen, H. N., 2014.** *Hydropower is still a concern for Gia Lai people in the rainy season*, *VietnamPlus*. <https://www.vietnamplus.vn/thuy-dien-van-la-moi-lo-cua-nguoi-dan-gia-lai-va-o-mua-mua-post267864.vnp> (in Vietnamese)
- Nguyen, T., Dong, N., & Huu, P., 2021.** *The Central Highlands - South Central region respond to the risk of desertification -Chapter 1: Water resource depletion*, <https://www.sggp.org.vn/tay-nguyen-nam-trung-bo-ung-pho-nguy-co-sa-mac-hoa-bai-1-suy-kiet-nguon-nuoc-post593524.html> (in Vietnamese)
- O’Neill, C., McCann, M., & Syam, U., 2023.** *America Is Draining Its Groundwater Like There’s No Tomorrow*. *The New York Times*. <https://www.nytimes.com/interactive/2023/08/28/climate/groundwater-drying-climate-change.html>
- Onyango, V., Masumbuko, B., Somda, J., Nianogo, A., & Davies, J., 2016.** *Sustainable Land Management in Rangeland and Grasslands*, <https://doi.org/10.4060/cc0852en>
- Owuor, S. O., Butterbach-Bahl, K., Guzha, A. C., Rufino, M. C., Pelster, D. E., Díaz-Pinés, E., & Breuer, L., 2016.** *Groundwater recharge rates and surface runoff response to land use and land cover changes in semi-arid environments*, *Ecological Processes*, 5(1), 1–21.  
<https://doi.org/10.1186/S13717-016-0060-6/TABLES/4>
- Phong, T., 2020.** *The risk of depletion and pollution of water sources in the Central Highlands*, *Vietnam Law Electronic Newspaper*. <https://baophapluat.vn/nguy-co-can-kiet-va-o-nhiem-nguon-nuoc-o-tay-nguyen-post376179.html> (in Vietnamese)
- Prucha, B., Graham, D., Watson, M., Avenant, M., Esterhuysen, S., Joubert, A., Kemp, M., King, J., Le Roux, P., Redelinghuys, N., Rossouw, L., Rowntree, K., Seaman, M., Sokolic, F., Van Rensburg, L., Van Der Waal, B., Van Tol, J., & Vos, T., 2016.** *MIKE-SHE integrated groundwater and surface water model used to simulate scenario hydrology for input to DRIFT-ARID: The Mokolo River case study*, *Water SA*, 42(3), 384–398.  
<https://doi.org/10.4314/wsa.v42i3.03>
- Salem, A., Abduljaleel, Y., Dezsó, J., & Lóczy, D., 2023.** *Integrated assessment of the impact of land use changes on groundwater recharge and groundwater level in the Drava floodplain, Hungary*, *Scientific Reports* 2023 13:1, 13(1), 1–16.  
<https://doi.org/10.1038/s41598-022-21259-4>
- Sandu, M.A., & Virsta, A., 2015.** *Applicability of MIKE SHE to Simulate Hydrology in Argesel River Catchment*, *Agriculture and Agricultural Science*

- Procedia, 6, 517–524.  
<https://doi.org/10.1016/j.aaspro.2015.08.135>
- Scanlon, B. R., Reedy, R. C., Stonestrom, D. A., Prudic, D. E., & Dennehy, K. F.,** 2005. *Impact of land use and land cover change on groundwater recharge and quality in the southwestern US*. *Global Change Biology*, 11(10), 1577–1593.  
<https://doi.org/10.1111/J.1365-2486.2005.01026.X>
- Scikit-learn,** 2023. 3.1. *Cross-validation: evaluating estimator performance — scikit-learn 1.3.2 documentation*, Scikit-Learn.Org. [https://scikit-learn.org/stable/modules/cross\\_validation.html](https://scikit-learn.org/stable/modules/cross_validation.html)
- Shannon, P. D., Swanston, C. W., Janowiak, M. K., Handler, S. D., Schmitt, K. M., Brandt, L. A., Butler-Leopold, P. R., & Ontl, T.,** 2019. *Adaptation strategies and approaches for forested watersheds*, *Climate Services*, 13, 51–64.  
<https://doi.org/10.1016/J.CLISER.2019.01.005>
- Shu, Y., Li, H., & Lei, Y.,** 2018. *Modelling groundwater flow with MIKE SHE using conventional climate data and satellite data as model forcing in Haihe Plain, China*, *Water (Switzerland)*, 10(10).  
<https://doi.org/10.3390/w10101295>
- Siddik, M. S., Tulip, S. S., Rahman, A., Islam, M. N., Haghghi, A. T., & Mustafa, S. M. T.,** 2022a. *The impact of land use and land cover change on groundwater recharge in northwestern Bangladesh*. *Journal of Environmental Management*, 315, 115130.  
<https://doi.org/10.1016/J.JENVMAN.2022.115130>
- Siddik, M. S., Tulip, S. S., Rahman, A., Islam, M. N., Haghghi, A. T., & Mustafa, S. M. T.,** 2022b. *The impact of land use and land cover change on groundwater recharge in northwestern Bangladesh*, *Journal of Environmental Management*, 315.  
<https://doi.org/10.1016/J.JENVMAN.2022.115130>
- Tran, H.,** 2019. *Drought threatens production in Gia Lai. Thanh Nien*, <https://thanhnien.vn/han-han-de-doa-san-xuat-o-gia-lai-185827955.htm> (in Vietnamese).
- Tuan, L.,** 2016. *Late 21st century: The risk of desertification in the Central Highlands*, Lam Dong Online. <https://baolamdong.vn/khoahoc/201604/cuoi-the-ky-21-nguy-co-bi-hoang-mac-hoa-tay-nguyen-2681101/> (in Vietnamese).
- USGS,** 2018. *Groundwater Use in the United States | U.S. Geological Survey*. [www.usgs.gov](http://www.usgs.gov).  
<https://www.usgs.gov/special-topics/water-science-school/science/groundwater-use-united-states>
- VAWR,** 2021. *Issues in the exploitation, use and management of underground water resources in the Central Highlands*, Vietnam Academy for Water Resources. <https://vawr.org.vn/cac-van-de-trong-viec-khai-thac-su-dung-va-quan-ly-nguon-tai-nguyen-nuoc-duoi-dat-vung-tay-nguyen> (in Vietnamese)
- VMHA,** 2020. *Strengthen natural disaster warnings to remote communities*. *Vietnam Meteorological and Hydrological Administration*.  
<http://vmha.gov.vn/cong-tac-pctt-tkc-130/tang-cuong-can-h-bao-thien-tai-toi-cong-dong-vung-sau-vung-xa-7050.html> (in Vietnamese)
- VWSA,** 2022. *Groundwater - A resource that needs protection*. Vietnam Water Supply and Sewerage Association.  
<http://vwsa.org.vn/vn/article/2405/nuoc-ngam-nguon-tai-nguyen-can-bao-ve.html> (in Vietnamese)
- Wakode, H. B., Baier, K., Jha, R., & Azzam, R.,** 2018. *Impact of urbanization on groundwater recharge and urban water balance for the city of Hyderabad, India*, *International Soil and Water Conservation Research*, 6(1), 51–62.  
<https://doi.org/10.1016/J.ISWCR.2017.10.003>
- Wang, L., Jia, B., Xie, Z., Wang, B., Liu, S., Li, R., Liu, B., Wang, Y., & Chen, S.,** 2022. *Impact of groundwater extraction on hydrological process over the Beijing-Tianjin-Hebei region, China*, *Journal of Hydrology*, 609, 127689.  
<https://doi.org/10.1016/J.JHYDROL.2022.127689>
- Wijsekara, G. N., Gupta, A., Valeo, C., Hasbani, J. G., & Marceau, D. J.,** 2010. *Impact of land-use changes on the hydrological processes in the Elbow river watershed in southern Alberta*, International Environmental Modelling and Software Society (IEMSS) 2010 International Congress on Environmental Modelling and Software Modelling for Environment's Sake, Fifth Biennial Meeting, Ottawa, Canada.  
<https://scholarsarchive.byu.edu/iemssconference>
- Wilcox, B. P., Le Maitre, D., Jobbagy, E., Wang, L., & Breshears, D. D.,** 2017. *Ecohydrology: Processes and Implications for Rangelands*, Springer Series on Environmental Management. Springer, Cham, 85–129. [https://doi.org/10.1007/978-3-319-46709-2\\_3](https://doi.org/10.1007/978-3-319-46709-2_3)
- Yadav, S. K., & Yadav, S. K.,** 2023. *Land Cover Change and Its Impact on Groundwater Resources: Findings and Recommendations*, IntechOpen.  
<https://doi.org/10.5772/INTECHOPEN.110311>
- Zhang, W., Zhu, X., Xiong, X., Wu, T., Zhou, S., Lie, Z., Jiang, X., & Liu, J.,** 2023. *Changes in soil infiltration and water flow paths: Insights from subtropical forest succession sequence*, *CATENA*, 221, 106748.  
<https://doi.org/10.1016/J.CATENA.2022.106748>

Received at: 18. 01. 2024

Revised at: 13. 03. 2024

Accepted for publication at: 19. 03. 2024

Published online at: 25. 03. 2024